Communication

One-Step low temperature synthesis of CeO_2 nanoparticles stabilized by carboxymethylcellulose

Vasily V. Spiridonov[1], Andrey V. Sybachin[1], Vladislava A. Pigareva[1], Mikhail I. Afanasov[1], Sharifjon A. Musoev[2], Alexander V. Knotko[2], Sergey B. Zezin[1]

[1] Lomonosov Moscow State University, Department of Chemistry, Leninskie gory 1-3, 119991, Moscow, Russia;
[2] Lomonosov Moscow State University, Faculty of Materials Science, Leninskie gory 1-73, 119991 Moscow, Russia;

Abstract: Nanocomposites consisting of cerium based nanoparticles stabilized by carboxymethyl cellulose (CMC) macromolecules were obtained using one-pot reaction at room temperature. The characterization of the nanocomposites was carried out with the use of combination of microscopy, XRD and IT-spectroscopy analysis. The type of crystal structure of inorganic nanoparticles corresponding to CeO_2 has been determined and the mechanism of the nanoparticles formation was suggested. It was demonstrated that the size and shape of nanoparticles in the resulting nanocomposites does not depend on the ratio of the initial reagents. Spherical particles with mean diameter 3 nm were obtained in different reaction mixtures. The scheme of the dual stabilization of CeO_2 nanoparticles with carboxylate and hydroxyl groups of CMC. These findings are promising for the development and application of Ce-based nanoparticles materials.

Keywords: carboxymethyl cellulose; cerium oxide; nanocomposite; cerium nanoparticles; stabilization; microscopy;

1. Introduction

Cerium-containing nanoparticles exhibiting biomimetic and antioxidant activity are now increasingly used in biology and medicine. For example, a high degree of biocompatibility, low toxicity, and catalytic activity of nanodispersed cerium dioxide make it possible to consider it as a promising material for biomedical applications [1, 2]. The influence of nanocrystalline cerium dioxide in the protection of living cells from oxidative stress was also found. The uniqueness of cerium dioxide nanoparticles is due to the fact that they can exist in different oxidation states: Ce^{3+} and Ce^{4+}, which distinguishes them from most other rare earth metals, which are predominantly in the trivalent state [3]. The nonstoichiometry of oxygen, associated with the ability to participate in redox processes in a living cell, as well as the ability to self-heal, ensures high efficiency in the use of nanodispersed cerium dioxide [4]. Moreover, the biological activity of cerium dioxide nanoparticles is determined by oxygen nonstoichiometry, which depends on the size of the nanoparticle and the nature of the surface ligand. The high degree of biocompatibility, low toxicity, and catalytic activity of nanodispersed cerium dioxide make it possible to consider it as a promising nanomaterial for biomedical applications. It has been shown that cerium-containing nanoparticles can act as superoxide dismutase, catalases, oxidases, and oxidoreductases. In this case, the efficiency of radical neutralization will always be proportional to the concentration of Ce3+ ions on the surface of nanoparticles. In addition, the size and state of the surface of CeO_2 particles determine the possibility of inactivation of superoxide free radicals, preventing oxidative stress in cells.

Preprints (www.preprints.org) | NOT PEER-REVIEWED | Posted: 9 February 2023 doi:10.20944/preprints202302.0168.v1

Another important property, the antioxidant activity of cerium oxide nanoparticles, is their dependence on the pH of the medium. Cerium oxide nanoparticles are able to most actively prevent oxidative stress in alkaline and neutral (physiological) media [5, 6].

To date, various methods have been proposed for obtaining cerium oxide nanoparticles: the sol-gel method, coprecipitation, microemulsion method, solvothermal and hydrothermal methods [7–11]. The key disadvantage of these methods for obtaining cerium-containing nanoparticles is the conduct of reactions at elevated temperatures, which leads to the formation of particles of arbitrary sizes, shapes, and the impossibility of controlling the geometric and morphological parameters of nanoparticles. Moreover, the problem of stabilization of cerium-containing nanoparticles from aggregation and precipitation also remains relevant. The most commonly used approach to stabilize cerium oxide nanoparticles is using surfactants [12]. A significant disadvantage of this approach is the impossibility of complete purification of the formed nanocomposites from surfactants and limits the use of such materials for biomedical purposes.

Polyelectrolytes are promising components for effective stabilization of cerium-containing nanoparticles. The efficiency of preventing aggregation can be achieved due to the ability of charged groups in the main chain to interact electrostatically with the surface of nanoparticles. In addition, the use of polyelectrolytes of natural origin as nanoparticle stabilizers makes it possible to obtain biocompatible nanocomposite materials. One such polyelectrolyte is the sodium salt of carboxymethyl cellulose (CMC).

The paper proposes an original method for the preparation of cerium oxide nanoparticles, which was carried out by reduction of the Ce^{4+} complex salt with sodium borohydride in the presence of CMC at room temperature under aerobic conditions. Nanocomposites with different contents of the inorganic phase were obtained. In the resulting nanocomposites, the content of the inorganic component was determined by UV-spectrophotometry. The nanocomposites were also characterized by TEM, SEM, XRD and IR spectroscopy. It was established that the size of nanoparticles in the composition of composites does not depend on the ratio of components in the reaction mixture and is 2.9±0.2 nm. It is shown that the type of crystal lattice of nanoparticles corresponds mainly to the structure of CeO2. A significant decrease in the size of macromolecules containing CeO_2 nanoparticles compared to the initial CMC macromolecules was found, and the values of the electrophoretic mobility of the nanocomposites were measured. It has been shown that both carboxyl and hydroxyl groups, which are part of CMC, play a role in the stabilization of nanoparticles.

2. Materials and Methods

2.1. Objects of study

The following reagents were used in the work: sodium salt of CMC with molecular mass 90.000 Da (Merck, USA), ammonium cerium nitrate, $(NH_4)_2Ce(NO_3)_6$ (Reakhim, Russia, Special Purification) and sodium borohydride (99%, Pulver, Belgium).

The synthesis of composite materials based on the sodium salt of carboxymethyl cellulose and cerium oxide nanoparticles was carried out according to the following procedure. To 2.5 ml of a 2% solution containing CMC was added dropwise from 6.3 to 17.6 mg of $(NH_4)_2Ce(NO_3)_6$ dissolved in 5 ml of water with vigorous stirring. Then, 0.5 ml of a $NaBH_4$ solution containing from 3 mg to 5 mg respectively were added, intensively stirring the resulting mixture. The total volume of the reaction mixture was 8 ml. The resulting solution was stirred for 12 hours. Then, within 12 hours, purification from low molecular weight components was carried out by dialysis (in dialysis bags Sigma, MWCO~12 kDa) against water for 24 hours. The resulting products were lyophilized.

2.2. Research Methods for Cerium-Containing Nanocomposites.

2.2.1. UV spectroscopy.

The determination of the cerium content in the composites was carried out using the UV spectroscopy method. The measurements were carried out on a Specord M40 device

Preprints (www.preprints.org) | NOT PEER-REVIEWED | Posted: 9 February 2023 doi:10.20944/preprints202302.0168.v1

from Carl Zeiss (Jena, Germany) in the spectral range from 280 to 500 nm. Sample solutions were prepared to record UV spectra. A calibration graph was built according to the method given in [13]. To construct this calibration graph, weighed amounts of cerium ammonium nitrate 0.5 mg, 1 mg, 1.5 mg and 2 mg were dissolved in 100 μl of concentrated H_2SO_4. Then 10 ml of an aqueous solution containing 0.1% wt. silver nitrate and 0.2 g ammonium persulfate was added to solutions. After that, the UV spectra of the obtained solutions were recorded in the wavelength range from 200 to 500 nm and the absorption intensity was measured at a wavelength of 310 nm, $D_{\lambda=310\ nm}$. Absorption spectra of solutions containing cerium ions of various concentrations and a calibration are presented in Supplementary materials Figure S1.

2.2.2. Transmission electron microscopy (TEM).

Structural studies were carried out by transmission (tunneling) electron microscopy (TEM) on a JEM-100B setup (JEML) equipped with an attachment for X-ray phase analysis. Samples were prepared by applying a drop of an aqueous solution containing the test substance to a copper grid with further drying in air atmosphere. The samples were examined without preliminary contrasting.

2.2.3. X-ray phase analysis (XRF).

X-ray studies were carried out on a Rigaku D/Max2500 diffractometer with a rotating anode (Japan). The survey was carried out in reflection mode (Bragg-Brentano geometry) using CuKav. radiation (cf. wavelength λ=1.54183 Å). Generator operation parameters: accelerating voltage 40 kV, tube current 200 mA. The survey was carried out in quartz cuvettes without averaging rotation. Solvents were not used to fix the powder samples. Recording parameters: angle interval $2\theta = 2° – 60°$, step (in 2θ) 0.02°, spectrum recording rate 5°/min. Silicon powder was used as an internal standard for correction.

Qualitative analysis of the obtained radiographs was performed using the WinXPOW software package using the ICDDPDF-2 database.

2.2.4. IR spectroscopy.

The nature of the interaction between the samples was studied by IR spectroscopy on a Specord M80 instrument (Carl Zeiss, Jena, Germany). Studies were carried out in the absorption mode by preparing tablets from KBr (matrix) and a carefully ground sample.

2.2.5. Raster (scanning) electron microscopy (SEM).

The microstructure of the samples was studied using a scanning electron microscope with a LEO SUPRA 50VP field emission source (Carl Zeiss, Germany). For the study, the samples were glued on a metal table using a conductive carbon adhesive tape and a layer of carbon or chromium was deposited on them (sputtering unit Quorum 150T - (UK), voltage 1000-1200 V, current strength 5-10 mA, deposition time 5-10 minutes. The accelerating voltage of the electron gun was 5–20 kV. Images were obtained in secondary electrons (detector SE2) at magnifications up to 100,000× and recorded in digitized form on a computer.

3. Results

An original technique was used for the first time to obtain CMC-CeO_2 nanocomposites. CMC-CeO_2 nanocomposites were obtained by treating CMC with solutions of $(NH_4)_2Ce(NO_3)_6$ and a reducing agent ($NaBH_4$) at room temperature. A feature of the proposed approach is the formation of cerium oxide in an aqueous medium simultaneously in the presence of a strong reducing agent and atmospheric oxygen. The need to use a reducing agent is due to the chemical specificity of this process, which, apparently, includes the following stages [14, 15]:

$$Ce^{4+} + BH_4^- \rightarrow Ce^{3+} + B(OH)_3 + H_2 \quad (1)$$

$$NaBH_4 + H_2O \rightarrow NaB(OH)_4 + H_2 \quad (2)$$

$$NaB(OH)_4 \rightarrow NaOH + B(OH)_3 \quad (3)$$

Preprints (www.preprints.org) | NOT PEER-REVIEWED | Posted: 9 February 2023 doi:10.20944/preprints202302.0168.v1

$$Ce^{3+} + 3OH^- \rightarrow Ce(OH)_3 \quad (4)$$

$$4Ce(OH)_3 + O_2 \rightarrow 4CeO_2 + 6H_2O \quad (5)$$

During the synthesis, the concentration of CMC was kept constant, while the concentration of the cerium salt, the source of cerium (IV) ions, changed 6-fold (see details in Table 1). This made it possible to trace the effect of the molar ratio of components in the reaction system on the composition of the final product.

Table 1. Composition of the reaction mixture for the synthesis of cerium-containing nanoparticles and Ce^{4+} yield.

[CMC], base-mole/L	$(NH_4)_2Ce(NO_3)_6$, mM	[CMC]/[Ce^{4+}]	Ce^{4+} in composite, wt. %*
0,08	0,002	20:1	6,4
0,08	0,0053	15:1	7,1
0,08	0,008	10:1	9,0
0,08	0,011	7:1	11,0
0,08	0,016	5:1	14,1

- Determined by UV-spectroscopy

The TEM method was used to visualize the inorganic particles included in the composition of the obtained substances (Figures 1-4). The figures presents TEM images of samples obtained at various [CMC]/[Ce^{4+}] ratios in the reaction mixture.

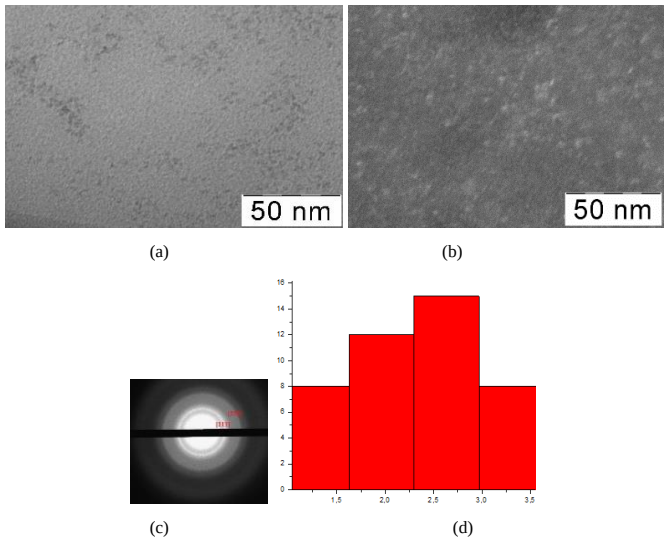

Figure 1. TEM-images (a), TEM-images in dark field (b), diffractogramms (c), nanoparticles size distribution (d) of nanoceria-containing composites of CMC with 6.4 wt.% Ce^{4+}

Preprints (www.preprints.org) | NOT PEER-REVIEWED | Posted: 9 February 2023 doi:10.20944/preprints202302.0168.v1

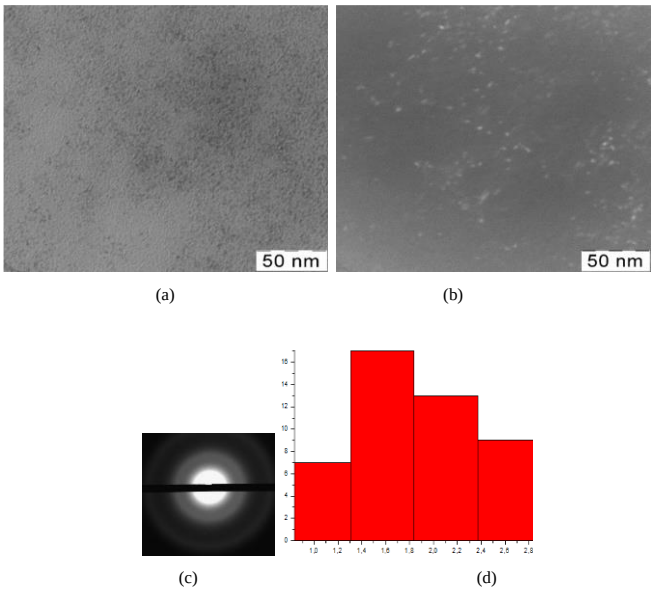

Figure 2. TEM-images (a), TEM-images in dark field (b), diffractogramms (c), nanoparticles size distribution (d) of nanoceria-containing composites of CMC with 7.1 wt.% Ce^{4+}

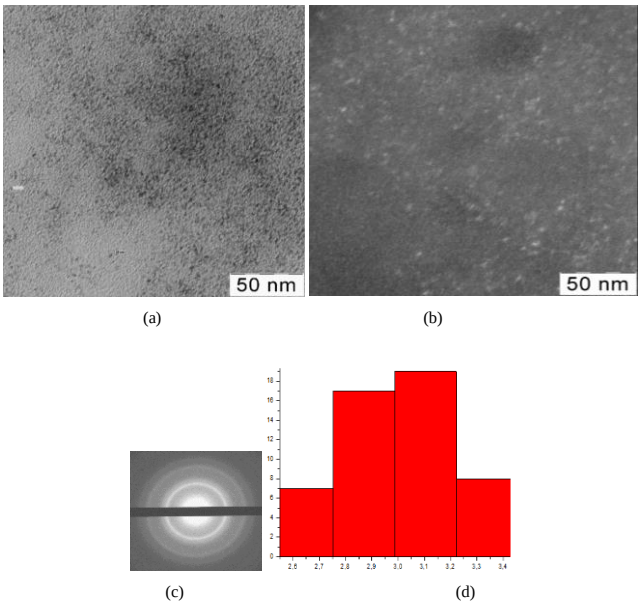

Figure 3. TEM-images (a), TEM-images in dark field (b), diffractogramms (c), nanoparticles size distribution (d) of nanoceria-containing composites of CMC with 9,0 wt.% Ce^{4+}

Preprints (www.preprints.org) | NOT PEER-REVIEWED | Posted: 9 February 2023 doi:10.20944/preprints202302.0168.v1

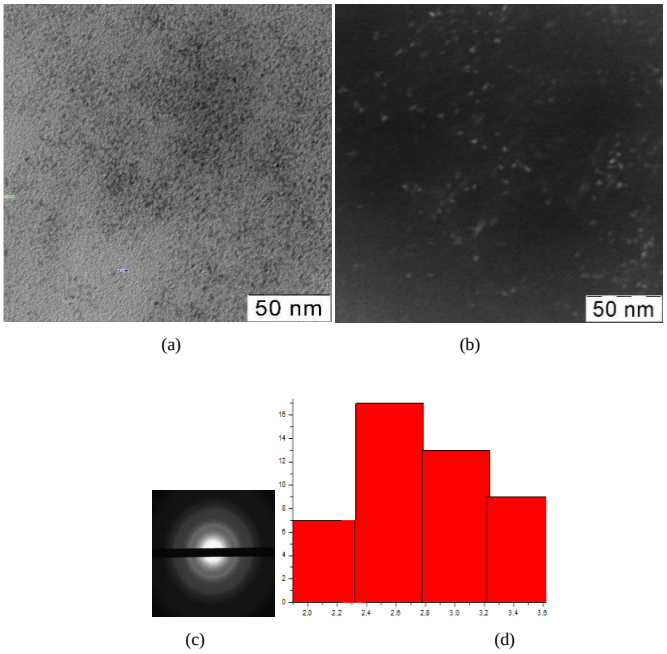

Figure 4. TEM-images (a), TEM-images in dark field (b), diffractogramms (c), nanoparticles size distribution (d) of nanoceria-containing composites of CMC with 11.0 wt. % Ce^{4+}

All presented TEM images demonstrate presence of dark contrasting nanometer-sized spherical particles. On dark-field TEM images of samples nanometer-sized particles appear as bright spots. This indicates that they have a crystalline structure and represent themselves as sources of diffraction. The presence of a crystalline structure in nanoparticles was confirmed by electron diffraction patterns, which could be described as a set of diffuse Bragg reflections.

Using TEM images, the sizes of spherical nanoparticles in composites was calculated. The resulted values in all the studied samples were in range 2.9 ± 0.2 nm. Thus, the ratio of components in the reaction mixture did not affect the shape and size of nanoparticles in the obtained products.

The identification of the crystal structure of the inorganic phase in cerium-containing products based on CMC was carried out using the XRD method (Figure 5).

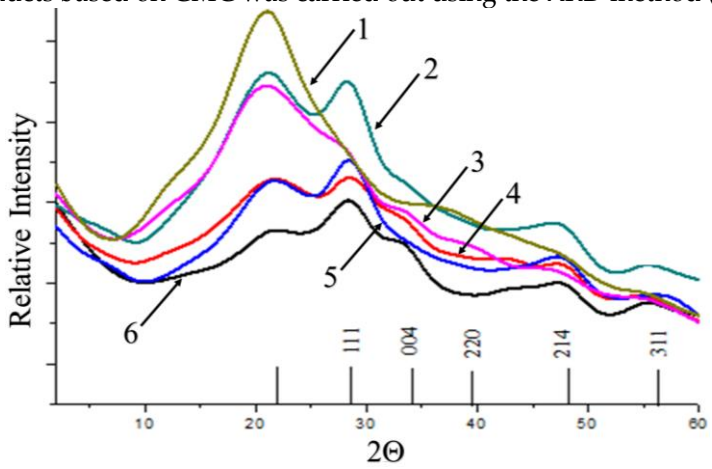

Figure 5. XRD patterns of cerium-containing products based on CMC: pure CMC (1), composite with 6.4 wt.% Ce^{4+} (2); composite with 7.1 wt.% Ce^{4+} (3); composite with 9 wt.% Ce^{4+} (4); composite with 11.0 wt. % Ce^{4+} (5); composite with 14.1 wt.% Ce^{4+} (6). XRD pattern of pure cerium oxide is presented as thin lines.

All diffractograms presented in Figure 6 curves 2-6 have peaks at angles 2θ = 28.4°, 34.38°, 47.6° and 57°. Broad reflections indicate a presence of small particle size of the inorganic phase. The diffraction pattern of the original CMC (Figure 6 curve 1) does not

Preprints (www.preprints.org) | NOT PEER-REVIEWED | Posted: 9 February 2023 doi:10.20944/preprints202302.0168.v1

contain these peaks. A comparative diffraction pattern of cerium oxide powder (thin lines) is presented to demonstrate that the positions of the cerium oxide peaks completely coincide with those for all obtained cerium-containing products based on CMC.

The microstructure of cerium-containing composites based on CMC was studied by SEM (Figure 6).

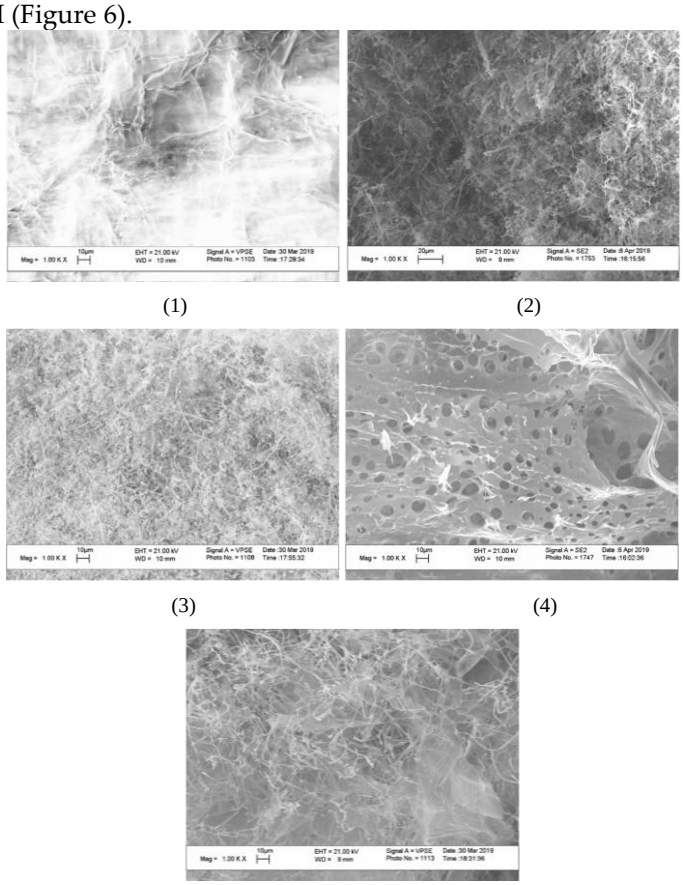

(1) (2)

(3) (4)

(5)

Figure 6. SEM-images of cerium-containing products based on CMC: composite with 6.4 wt.% Ce^{4+} (1); composite with 7.1 wt.% Ce^{4+} (2); composite with 9 wt.% Ce^{4+} (3); composite with 11.0 wt. % Ce^{4+} (4); composite with 14.1 wt.% Ce^{4+} (5).

The image of plane surface was obtained by SEM in characterizing of initial CMC. The appearance of CeO_2 nanoparticles in the content of composites leads to the formation of a porous structure. The pore sizes were practically independent on the mass content of CeO_2 nanoparticles and varied from 4 to 10 μm.

The nature of interactions between CMC macromolecules and cerium oxide nanoparticles was studied by IR spectroscopy (Figure 7).

Preprints (www.preprints.org) | NOT PEER-REVIEWED | Posted: 9 February 2023 doi:10.20944/preprints202302.0168.v1

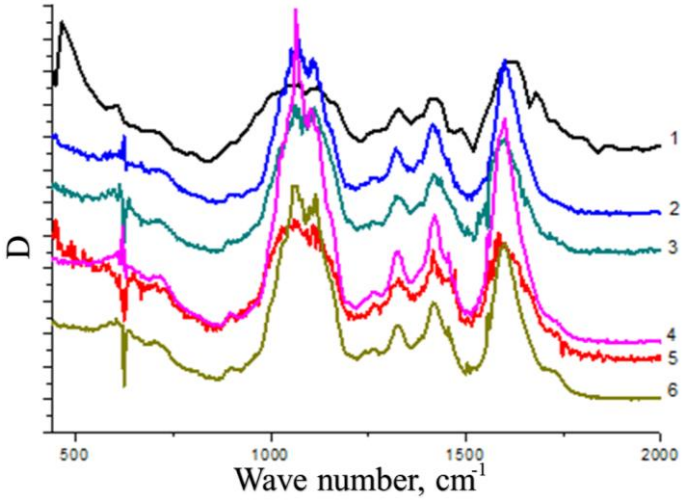

Figure 7. IR spectra of cerium-containing products based on CMC: pure CMC (1), composite with 6.4 wt.% Ce^{4+} (2); composite with 7.1 wt.% Ce^{4+} (3); composite with 9 wt.% Ce^{4+} (4); composite with 11.0 wt. % Ce^{4+} (5); composite with 14.1 wt.% Ce^{4+} (6).

CMC spectrum contains bands at wavelengths ν= 1688 cm^{-1} and ν = 1410 cm^{-1}, related to antisymmetric and symmetric stretching vibrations of the carboxyl groups of the polyanion, respectively. It should be noted a wide peak in the range of 1690–1740 cm^{-1}, corresponding to the stretching vibrations of the C=O group in the composition of the carboxyl groups of the polyanion. It is known that the presence of the C=O group in the composition of CMC indicates the formation of a system of intra- and intermolecular hydrogen bonds with its participation [16]. In addition, in the CMC spectrum there is a band at ν = 1220 cm^{-1}, associated with out-of-plane bending vibrations of the hydroxyl groups of the polysaccharide.

In the spectra of nanocomposites, as the cerium content increases, the absorption decreases in the range of 1690–1740 cm^{-1}. This phenomenon is associated with a violation of the internal structure of the CMC, accompanied by the destruction of the system of hydrogen bonds and the formation of electrostatic contacts between the carboxyl groups of the polysaccharide and the surface of the nanoparticles. In the spectra of nanocomposites, a shift of the band at ν = 1688 cm^{-1} to the region of lower wave numbers up to ν = 1668 cm^{-1} is observed. The shift of this band is additional evidence that some of the carboxyl groups of the polyanion are involved in electrostatic interaction with the surface of cerium oxide nanoparticles. Simultaneously, there is a decrease in the intensity of the band at ν =1220 cm^{-1}. The observed phenomenon indicates that some of the hydroxyl groups of the polyanion do not realize out-of-plane bending vibrations. These hydroxyl groups take part in the interaction with the particles of the inorganic phase, forming coordination bonds with cerium ions on the surface of the nanoparticles.

Thus, nanoparticles are included in the composition of the polymer matrix due to the implementation of interactions between surface cerium ions and functional groups of carboxymethyl cellulose. Carboxyl groups of the polysaccharide form electrostatic contacts with nanoparticles. In addition, formation of composite results in destruction of the system of hydrogen bonds with the participation of carboxyl groups of the initial CMC. Due to this effect the formation of a system of coordination bonds between the hydroxyl groups of polysaccharides and cerium ions on the surface of nanoparticles is possible. That. In turn, is an additional factor that increases the stability of nanoparticles and their aggregative stability. The scheme of the stabilized nanoparticles is presented on the Figure 8.

Preprints (www.preprints.org) | NOT PEER-REVIEWED | Posted: 9 February 2023 doi:10.20944/preprints202302.0168.v1

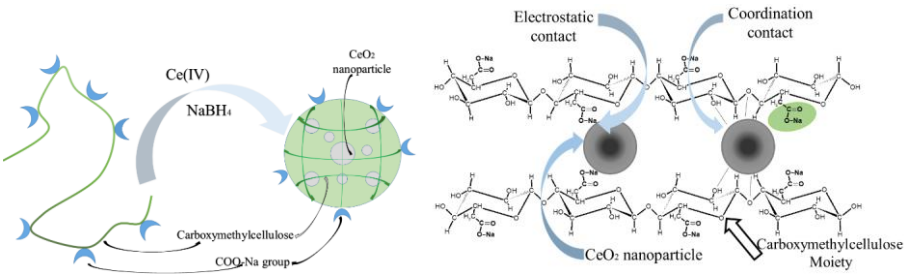

(a) (b)

Figure 8. Scheme of formation of the CMC-CeO_2 composite (a); Electrostatic and coordination bonds formation between polysaccharide and surface of cerium oxide nanoparticles (b).

4. Discussion

A one-pot synthesis of fine dispersed CeO_2 nanoparticles could be carried out at room temperature by direct synthesis in solution of CMC. The formation of nanoparticles occurs in several stages. First, cerium (IV) from the dissolved $(NH_4)_2Ce(NO_3)_6$ undergoes reduction to cerium (III) in form of cerium hydroxide which undergoes oxidation by air oxygen dissolved in water. Grows of the nanoparticles is restricted by stabilizing agent- CMC. Using different CMC-to-cerium molar ratio it was demonstrated that the almost spherical particles with average mean diameter 3 nm were formed in all studied reaction mixtures. Such behavior could be attributed to limitation of the process of nanoparticle formation by the study of particle grows restricted with effective stabilization of the surface with groups of CMC. In compare, the formation of maghemite particles in presence of CMC matrix results in formation of bigger nanoparticles with average size 10-12 nm and relatively broad dispersion [16].

The XRD analysis confirmed that the nanoparticles are crystals if CeO_2. Crystallinity of the polymer matrix in presence of nanoparticles decreased due to partial violation of structures stabilized by hydrogen bonds and disturbing of ordered structures by incorporation of nanoparticles. As a result, on SEM images the flat film of pure CMC transforms into porous film of CMC- cerium oxide nanocomposites.

To understand the nature of the stabilizing of CeO_2 nanoparticles with CMC the IR-spectroscopy was applied. We suggest that geometrically surrounded nanoparticles of cerium oxide are stabilized with both carboxylate and hydroxyl groups of CMC. The first one ensures electrostatic stabilization while the second one is responsible for the coordination contacts. Dual action of these groups results in effective stabilization of the nanoparticles with relatively small size.

5. Conclusions

Nanocomposites consisting of CeO_2 nanoparticles stabilized by carboxymethyl cellulose macromolecules were obtained. It has been found that varying the ratio of the components of the reaction mixture in the course of synthesis makes it possible to obtain nanocomposites with different contents of the inorganic phase while the size and morphology of the nanoparticles did not depend on the reaction mixture composition. Nanoparticles had spherical shape with average diameter 3 nm. The type of crystal structure of inorganic nanoparticles in nanocomposites corresponding to CeO_2 has been confirmed with XRD. It has been demonstrated that stabilization of the nanoparticles is attributed to electrostatic and coordination contacts with macromolecules. These findings could be useful for the further development and application of the cerium oxide nanoparticles.

Supplementary Materials: The following supporting information can be downloaded at: www.mdpi.com/xxx/s1, Figure S1: title; Table S1: title; Video S1: title.

Author Contributions: Conceptualization, V.V.S.; methodology, M.I.A., A.V.K., S.B.Z.; validation, V.V.S,; formal analysis, V.V.S.; investigation, V.V.S., S.A.M.,V.A.P., S.B.Z., A.V.S.; resources, V.V.S.;

data curation, V.V.S.; writing—original draft preparation, V.V.S.; writing—review and editing, A.V.S.; visualization, V.V.S.; supervision, V.V.S.; project administration, V.V.S.; funding acquisition, V.V.S. All authors have read and agreed to the published version of the manuscript." Please turn to the CRediT taxonomy for the term explanation. Authorship must be limited to those who have contributed substantially to the work reported.

Funding: This research was supported by

Institutional Review Board Statement: Not applicable

Data Availability Statement: Not applicable.

Conflicts of Interest: The authors declare no conflict of interest.

References

1. Thakur, N.; Manna, P.; Das, J. Synthesis and biomedical applications of nanoceria, a redox active nanoparticle. *Journal of Nanobiotechnology* **2019**, 17, 84.

2. Saifi, M. A.; Seal, S.; Godugu, C.. Nanoceria, the versatile nanoparticles: Promising biomedical applications. *Journal of Controlled Release* **2021**, 338, 164–189.

3. Karakoti, A. S.; Monteiro-Riviere, N. A.; Aggarwal, R.; Davis, J. P.; Narayan, R. J.; Self, W. T.; Seal, S. Nanoceria as antioxidant: Synthesis and biomedical applications. *JOM* **2008**, 60(3), 33–37.

4. Habib, S.; Fayyad, E.; Nawaz, M.; Khan, A.; Shakoor, R. A.; Kahraman, R.; Abdullah, A. Cerium Dioxide Nanoparticles as Smart Carriers for Self-Healing Coatings. *Nanomaterials* **2020**, 10(4), 791.

5. Nelson, B.; Johnson, M.; Walker, M.; Riley, K.; Sims, C. Antioxidant Cerium Oxide Nanoparticles in Biology and Medicine. *Antioxidants* **2016**, 5(2), 15.

6. Alpaslan, E.; Yazici, H.; Golshan, N. H.; Ziemer, K. S.; Webster, T. J. pH-Dependent Activity of Dextran-Coated Cerium Oxide Nanoparticles on Prohibiting Osteosarcoma Cell Proliferation. *ACS Biomaterials Science & Engineering* **2015**, 1(11), 1096–1103.

7. Hosseini, M.; Amjadi, I.; Mohajeri, M.; Mozafari, M. Sol–Gel Synthesis, Physico-Chemical and Biological Characterization of Cerium Oxide/Polyallylamine Nanoparticles. *Polymers* **2020**, 12(7), 1444.

8. Pujar, M. S., Hunagund, S. M., Desai, V. R., Patil, S., Sidarai, A. H. (2018). One-step synthesis and characterizations of cerium oxide nanoparticles in an ambient temperature via Co-precipitation method, *AIP Conference Proceedings* **2018**, 1942, 050026.

9. Kockrick, E.; Schrage, C.; Grigas, A.; Geiger, D.; Kaskel, S. Synthesis and catalytic properties of microemulsion-derived cerium oxide nanoparticles. *Journal of Solid State Chemistry* **2008**, 181(7), 1614–1620.

10. Walton, R. I. Solvothermal synthesis of cerium oxides. *Progress in Crystal Growth and Characterization of Materials* **2011**, 57(4), 93–108.

11. Maria Magdalane, C.; Kaviyarasu, K.; Siddhardha, B.; Ramalingam, G. Synthesis and characterization of CeO_2 nanoparticles by hydrothermal method. *Materials Today: Proceedings*. **2020**.

12. Bumajdad, A.; Eastoe, J.; Mathew, A. Cerium oxide nanoparticles prepared in self-assembled systems. *Advances in Colloid and Interface Science* **2009**, 147-148, 56–66.

13. I D Nickson, I. D.; Boxall, C.; Jackson, A.; Whillock, G O H. A spectrophotometric study of cerium IV and chromium VI species in nuclear fuel reprocessing process streams, *Materials Science and Engineering* **2010**, 9, 012011.

14. Glavee, G. N.; Klabunde, K. J.; Sorensen, C. M.; Hadjapanayis, G. C. Borohydride reductions of metal ions. A new understanding of the chemistry leading to nanoscale particles of metals, borides, and metal borates. *Langmuir* **1992**, 8(3), 771–773.

15. Calvache-Muñoz, J.; Prado, F. A.; Rodríguez-Páez, J. E.; Cerium oxide nanoparticles: Synthesis, characterization and tentative mechanism of particle formation. *Colloids and Surfaces A: Physicochemical and Engineering Aspects* **2017**, 529, 146–159.

 doi:10.20944/preprints202302.0168.v1

16. Spiridonov, V. V.; Panova, I. G.; Makarova, L. A.; Afanasov, M. I.; Zezin, S. B.; Sybachin, A. V.; Yaroslavov, A. A. The one-step synthesis of polymer-based magnetic γ-Fe_2O_3-carboxymethyl cellulose nanocomposites. *Carbohydrate Polymers* **2017**, 177, 269–274.

17. Cuba-Chiem, L. T.; Huynh, L.; Ralston, J.; Beattie, D. A. In Situ Particle Film ATR FTIR Spectroscopy of Carboxymethyl Cellulose Adsorption on Talc: Binding Mechanism, pH Effects, and Adsorption Kinetics. *Langmuir* **2008**, 24(15), 8036–8044.